NASA TECHNICAL NOTE

NASA TN D-4602

INVESTIGATION OF THE EFFECT OF WHEEL BRAKING ON SIDE-FORCE CAPABILITY OF A PNEUMATIC TIRE

by Thomas A. Byrdsong

Langley Research Center
Langley Station, Hampton, Va.

NATIONAL AERONAUTICS AND SPACE ADMINISTRATION • WASHINGTON, D. C. • JUNE 1968

NASA TN D-4602

INVESTIGATION OF THE EFFECT OF WHEEL BRAKING ON SIDE-FORCE CAPABILITY OF A PNEUMATIC TIRE

By Thomas A. Byrdsong

Langley Research Center
Langley Station, Hampton, Va.

NATIONAL AERONAUTICS AND SPACE ADMINISTRATION

For sale by the Clearinghouse for Federal Scientific and Technical Information
Springfield, Virginia 22151 – CFSTI price $3.00

INVESTIGATION OF THE EFFECT OF WHEEL BRAKING ON SIDE-FORCE CAPABILITY OF A PNEUMATIC TIRE

By Thomas A. Byrdsong
Langley Research Center

SUMMARY

An experimental investigation was made to determine the effects of wheel braking on the side-force capability of a pneumatic tire. Data were obtained from tests of a smooth-tread pneumatic tire with an inflation pressure of 30 pounds per square inch (20.7 N/cm^2) at ground speeds of 10, 20, and 30 miles per hour (8.7, 17.4, and 26.1 knots) at wheel yaw angles of 4^o and 8^o on both wet and dry paved surfaces. The results indicate that a considerable amount of side-force capability is available during wheel braking in the slip-ratio range from free rolling to maximum braking force. For additional wheel braking, the side force decreases rapidly to zero at full skid.

INTRODUCTION

Research is currently being directed toward improving the control of airplanes while operating on runways. Much of this research has been devoted to airplane braking performance on slippery paved surfaces with particular emphasis on stopping effectiveness. (See, for example, ref. 1.) In some cases airplanes have gone off the side of the runway while brakes were being applied; this indicated a loss in steering capability. (See ref. 2.)

In an effort to obtain an insight into the effect of wheel braking on directional control, an experimental investigation was conducted to determine the side-force or cornering capability of a pneumatic tire during brake application. Tests were made with an automobile tire at forward speeds of 10, 20, and 30 miles per hour (8.7, 17.4, and 26.1 knots) on both wet and dry paved surfaces. This paper presents the variations of the drag-force and side-force friction coefficients (or braking- and cornering-force coefficients) throughout the slip-ratio range (from free rolling to the locked-wheel-skid condition) for yaw angles of 4^o and 8^o.

SYMBOLS

F_x	ground force parallel to direction of motion, pounds (newtons)
$F_{D,\psi}$	ground force parallel to test-wheel plane, pounds (newtons)
F_y	ground force perpendicular to direction of motion, pounds (newtons)
F_ψ	ground force perpendicular to test-wheel plane, pounds (newtons)
F_z	vertical load on test tire, pounds (newtons)
r	rolling radius of test tire, feet (meters)
r_t	rolling radius of trailing-wheel tire, feet (meters) (see fig. 1(a))
s	wheel slip ratio, $1 - \frac{r\omega}{V}$
V	ground velocity of test vehicle, miles per hour (knots)
μ_x	drag-force friction coefficient, $\frac{F_x}{F_z}$
$\mu_{x,max}$	maximum drag-force friction coefficient
μ_y	side-force friction coefficient, $\frac{F_y}{F_z}$
$\mu_{y,f}$	free-rolling side-force friction coefficient
ψ	yaw angle, degrees
ω	angular velocity of test wheel, radians per second
ω_t	angular velocity of trailing wheel, radians per second

APPARATUS AND TEST PROCEDURE

A smooth-synthetic-rubber-tread 7.75 × 14 bias-ply automobile tire having a free diameter of 2.29 feet (0.70 meter) and an inflation pressure of 30 pounds per square inch (20.7 N/cm2) was used in the tests. The wheel and tire were mounted on a test fixture and attached to a $2\frac{1}{2}$-ton (2.27 Mg) truck. (See figs. 1(a) to 1(c).) The test

fixture was located forward of and in line with the right front wheel of the truck. A drawing of the side and front views of the test fixture is shown in figure 1(d). The test fixture included a three-component force balance which measured the vertical load and the horizontal forces parallel and perpendicular to the wheel plane. The test wheel was equipped with a standard automobile shoe-type self-energizing brake. Pressure to be applied to the brake and the brake's rate of rise were adjusted prior to the tests. The vertical load, the magnitude of which could also be selected prior to the tests, was applied to the tire by two pneumatic cylinders on the test fixture (figs. 1(b) and 1(d)). These pneumatic cylinders were also used to lower the wheel onto the test surface and then to raise it from the surface at the end of each test. These cylinders were actuated by a manually operated switch in the truck. Fixed yaw angles could be obtained by rotating the test wheel and tire about a vertical axis and then locking it at the desired position.

The area selected for the tests was a smooth level concrete roadway long enough to allow the truck to reach the desired velocity prior to entering the selected test section. Part of this test section was flooded with water to a depth of approximately 1/2 inch (1.27 cm).

In the tests the truck was accelerated until it attained the specified speed. The pneumatic cylinders were then actuated and forced the wheel down onto the roadway. The wheel and tire were permitted to free roll for a short time under a vertical load of 1000 pounds (4.45 kN) to allow the transient forces generated during initial tire-surface contact to die out. Brake pressure was applied until the test wheel reached a fully locked condition. This procedure was repeated for ground speeds of 10, 20, and 30 miles per hour (8.7, 17.4, and 26.1 knots) at yaw angles of 4° and 8°. Data were obtained for complete brake cycles (from free rolling to the locked-wheel condition) on both dry and wet surfaces.

INSTRUMENTATION

Instrumentation was provided to obtain time histories of the forces and motion. The vertical force and the horizontal forces parallel and perpendicular to the wheel plane were measured by the three-component force balance of the test fixture. Figure 1(e) is a photograph of the force balance removed from the test fixture and shows the locations of the electrical strain gages used to measure the applied loads. Although no significant interaction error was observed between the horizontal- and vertical-force components, an interaction error of about 3 percent was present in the measurements of the horizontal components. This error was corrected out in the data-reduction process.

Angular velocity of the test wheel was obtained by use of a direct-current generator. The outer case of the generator was attached to the test fixture, and the shaft was geared to the wheel.

The linear velocity of the test wheel was considered to be the same as the truck velocity. The truck velocity was obtained by means of the trailing wheel which was attached to the rear of the truck (fig. 1(a)). A magnetic pickup attached to the trailing wheel indicated wheel angular displacement with time, and the truck velocity was then obtained from the product of the trailing-wheel angular velocity and rolling radius.

The yoke that joined the trailing wheel to the truck was free to swivel about a vertical axis at the truck attachment point. The motion of the yoke with respect to the truck was measured by a potentiometer to indicate any significant departures of the truck from straight-line motion during a braking test.

Test-wheel brake pressure was measured by a pressure transducer in the hydraulic line which supplied pressure to the brake.

The effects of acceleration on the forces measured by the three-component force balance were obtained from three accelerometers mounted near the center of the wheel axle. (See fig. 1(c).)

The outputs of all instrumentation were recorded on a galvanometer-type recording oscillograph.

RESULTS AND DISCUSSION

If a braking torque is applied to a rolling wheel and the wheel is yawed with respect to its direction of motion, the angle of the resultant-force vector at the tire-ground interface will not be alined with the direction of motion. This misalinement is caused primarily by the side-force component developed by the tire under the yawed-rolling condition. The braking or stopping performance of a vehicle depends on the component of force along the direction of vehicle motion, whereas the steering or cornering capability depends on the component of force perpendicular to the direction of vehicle motion. The force components at the ground parallel and perpendicular to the wheel plane were actually measured by the balance. The measured forces were converted into components parallel and perpendicular to the direction of motion by using the following trigonometric transformations, which are illustrated vectorially in figure 2:

$$F_X = F_{D,\psi} \cos \psi + F_\psi \sin \psi$$

$$F_Y = F_\psi \cos \psi - F_{D,\psi} \sin \psi$$

In figure 3 are presented typical time histories of test-wheel angular velocity, brake pressure, and drag-force and side-force friction coefficients obtained during a dry-surface test at a yaw angle of 4° and ground speed of 20 miles per hour (17.4 knots).

During the first 1/2 second, no brake pressure was applied as indicated by the zero value of the brake-pressure trace, and the wheel was in a free-rolling condition. During this initial time interval, the test-wheel angular velocity and the side-force friction coefficient were at the maximum steady-state values obtained during the test. The small value of drag-force friction coefficient indicated during this interval results from the rolling resistance plus the component of side force F_ψ in the drag direction. Following this initial free-rolling period, brake pressure was applied and the drag-force friction coefficient increased to a maximum value about 1.2 seconds after brake-pressure application. During the interval from the end of free rolling to the attainment of maximum drag-force friction coefficient, only a slight decrease occurred in both the wheel angular velocity and the side-force friction coefficient. Brake pressure was allowed to increase following the attainment of peak drag, and the drag-force friction coefficient then decreased until the wheel reached a fully locked condition. Instrumentation provided to measure deviation of truck motion from a straight line indicated no significant deviations during the test. This characteristic variation of the drag-force friction coefficient during the braking process is well known and has been discussed in a number of papers. (See, for example, ref. 3.) During the time interval following the attainment of maximum drag-force friction coefficient, the side-force friction coefficient decreased rapidly until a near-zero value was reached when the wheel was fully locked. This decrease would indicate that steering capability during braking for this test was relatively high prior to the attainment of the maximum drag-force friction coefficient but decayed rapidly as the wheel was braked to a full-skid condition.

The variations of the side- and drag-force friction coefficients with slip ratio are presented for ground speeds of 10, 20, and 30 miles per hour (8.7, 17.4, and 26.1 knots) at yaw angles of 4° (fig. 4) and 8° (fig. 5). These data were obtained on both dry and wet concrete surfaces. Steady-state values of the force coefficients were obtained prior to brake application and subsequent to wheel lockup.

The application of brake pressure was adjusted to provide a low wheel-spin-down rate. This adjustment reduced the effect of inertia forces on the balance measurements to a negligible value.

Slip ratio is defined herein as follows:

$$s = 1 - \frac{r\omega}{V}$$

For a freely rolling unbraked wheel, the slip ratio is zero. When sufficient braking torque is applied to lock the wheel, the slip ratio is unity. For the present data, however, the slip ratio was computed from the following equivalent equation:

$$s = 1 - \left(\frac{\omega}{\omega_t}\right)\left(\frac{r}{r_t}\right)$$

As shown in figures 4 and 5, the variation of the side-force friction coefficient with slip ratio on both dry and wet surfaces for both yaw angles and for the velocity range covered by these tests is much the same as that indicated by the time history of figure 3; that is, the side-force friction coefficient is a maximum during the free-rolling period (s = 0) and decreases to about zero when the wheel is braked to a locked-wheel skid (s = 1.0). The data of figures 4 and 5 indicate that a significant amount of the free-rolling side-force friction coefficient is available for steering in the slip-ratio range in which the braking coefficients rise from zero to their maximum value. For the dry surface, when maximum braking force was being developed, the smallest side-force friction coefficient obtained was about 75 percent of the free-rolling value; for the wet surface, the smallest side-force friction coefficient was about 50 percent of the free-rolling value. At the higher velocities on both wet and dry surfaces, the side-force friction coefficient decreased more rapidly subsequent to the occurrence of maximum drag-force friction coefficient. These data, therefore, indicate that in order to maintain significant steering capability during braking, particularly at the higher speeds, wheel braking should be controlled so as not to exceed the slip ratio at which the maximum drag-force friction coefficient occurred.

The variation of the free-rolling side-force friction coefficient and the maximum drag-force friction coefficient with ground speed for the data of figures 4 and 5 are presented in figure 6. The data indicate that as the speed increased, the free-rolling side-force friction coefficient obtained on dry surfaces remained essentially the same for each yaw angle. For the wet-surface, the side-force friction coefficient decreased as the speed increased. For example, at 10 miles per hour (8.7 knots) little difference was noted in the side-force friction coefficients obtained on dry and wet surfaces for both yaw angles. At 30 miles per hour (26.1 knots), however, the free-rolling side-force friction coefficient obtained on the wet surface was about one-half that obtained on the dry surface. This reduction in free-rolling side-force friction coefficient with increasing speed on wet surfaces was also reported in reference 4 and was attributed to the phenomenon of pneumatic-tire hydroplaning (ref. (5)). Furthermore, the free-rolling steady-state side-force friction coefficients for the dry surface and yaw angle of 8° (fig. 5) are larger than those for the dry surface and yaw angle of 4° (fig. 4) as would be expected. The free-rolling side-force friction coefficients for a yaw angle of 8° being almost the same as the maximum drag-force friction coefficients indicates that the free-rolling side-force friction coefficient is the maximum side-force friction coefficient. The present data agree with the data of reference 3 which indicated that the maximum free-rolling side-force and maximum drag-force friction coefficients were equal.

Experimental results presented in reference 6 indicate that synthetic rubber has higher maximum coefficients of friction than natural rubber. Airplane tires are generally constructed of natural rubber. The data contained in this paper were obtained from tests

of an automobile tire made of synthetic rubber; therefore, the actual friction coefficients presented in figures 4 and 5 may be somewhat higher than those obtained with natural-rubber airplane tires under the same conditions. The variations of cornering force with braking force can, however, be considered applicable to airplane tires.

CONCLUDING REMARKS

Braked cornering tests were made with a smooth-synthetic-rubber-tread 7.75×14 bias-ply automobile tire with an inflation pressure of 30 pounds per square inch (20.7 N/cm^2) at forward speeds of 10, 20, and 30 miles per hour (8.7, 17.4, and 26.1 knots) at yaw angles of 4^o and 8^o on both dry and wet paved surfaces. The results indicated that in order to maintain significant steering capability during braking on dry and wet pavements, particularly at higher speeds, it is highly desirable to control wheel braking so as not to exceed the slip ratio at which the maximum drag-force friction coefficient occurred. Further increases in slip ratio resulted in significant reductions in tire side-force capability. The results also indicated that at a ground speed of 10 miles per hour (8.7 knots), the surface condition had little effect on the free-rolling side-force friction coefficient. At a ground speed of 30 miles per hour (26.1 knots), however, a significant reduction in side-force friction coefficient occurred for operation on the wet surface as compared with operation on the dry surface.

Langley Research Center,
National Aeronautics and Space Administration,
Langley Station, Hampton, Va. February 20, 1968,
126-61-05-05-23.

REFERENCES

1. Horne, Walter B.; and Joyner, Upshur T.: Pneumatic Tire Hydroplaning and Some Effects on Vehicle Performance. [Preprint] 970 C, Soc. Automotive Eng., Jan. 1965.

2. Horne, Walter B.; and Joyner, Upshur T.: Traction of Pneumatic Tires on Wet Runways. Conference on Aircraft Operating Problems, NASA SP-83, 1965, pp. 9-17.

3. Smiley, Robert F.; and Horne, Walter B.: Mechanical Properties of Pneumatic Tires With Special Reference to Modern Aircraft Tires. NASA TR R-64, 1960. (Supersedes NACA TN 4110.)

4. Harrin, Eziaslav N.: Low Tire Friction and Cornering Forces on a Wet Surface. NACA TN 4406, 1958.

5. Horne, Walter B.; and Dreher, Robert C.: Phenomena of Pneumatic Tire Hydroplaning. NASA TN D-2056, 1963.

6. Maycock, G.: Studies on the Skidding Resistance of Passenger-Car Tyres on Wet Surfaces. Proc. Auto. Div. Inst. Mech. Eng. (London), vol. 180, pt. 2A, no. 4, 1965-1966, pp. 122-141.

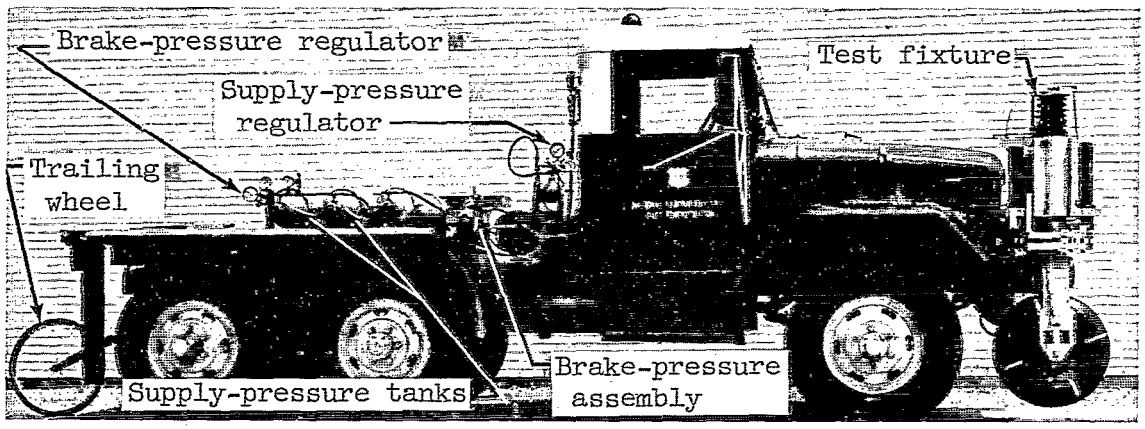

(a) Side view of test vehicle.

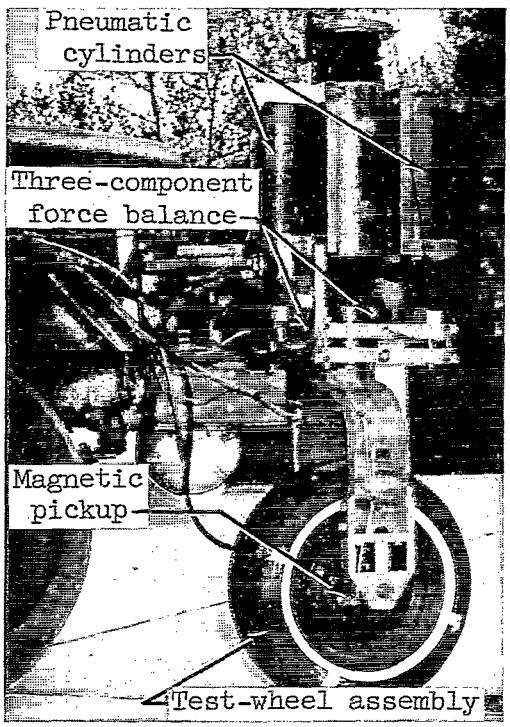

(b) Side view of test fixture.

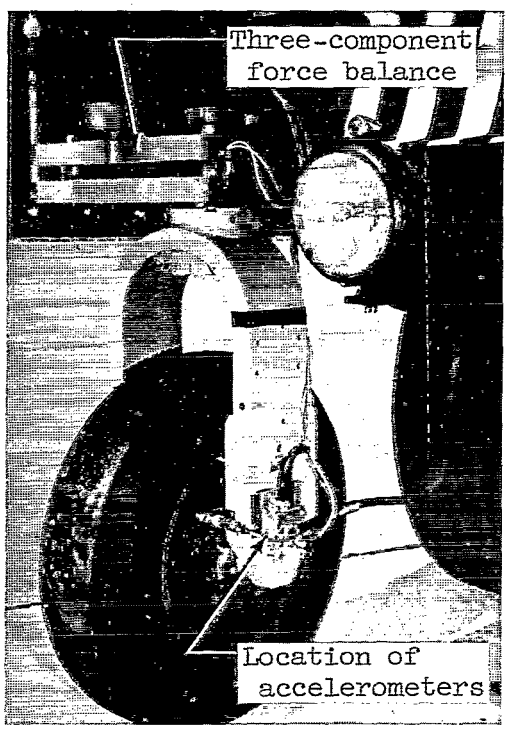

(c) Front view of test fixture.

Figure 1.- Views of test vehicle, test fixture, and three-component force balance. L-68-845

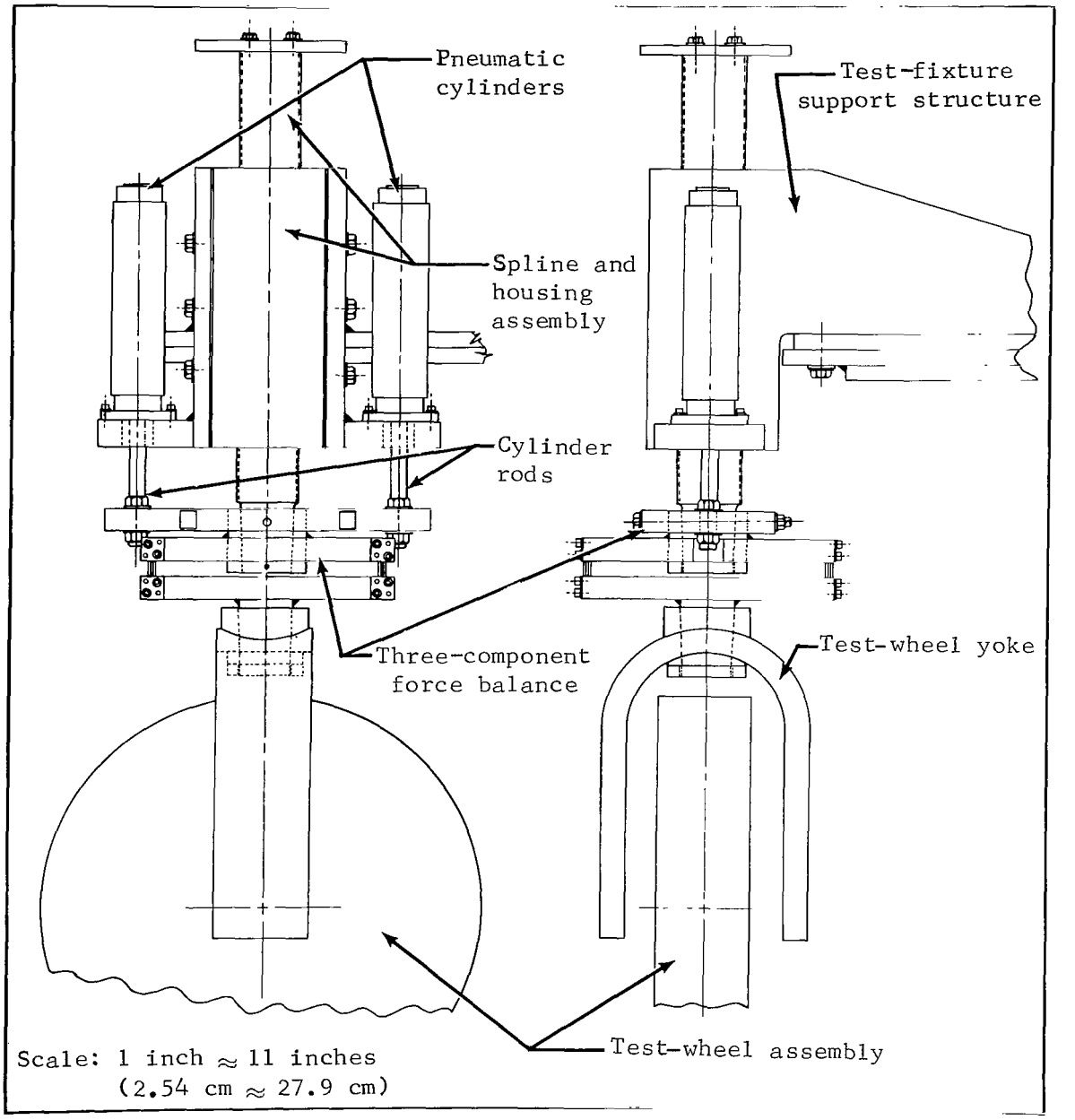

(d) Side- and front-view drawing of test fixture.

Figure 1.- Continued.

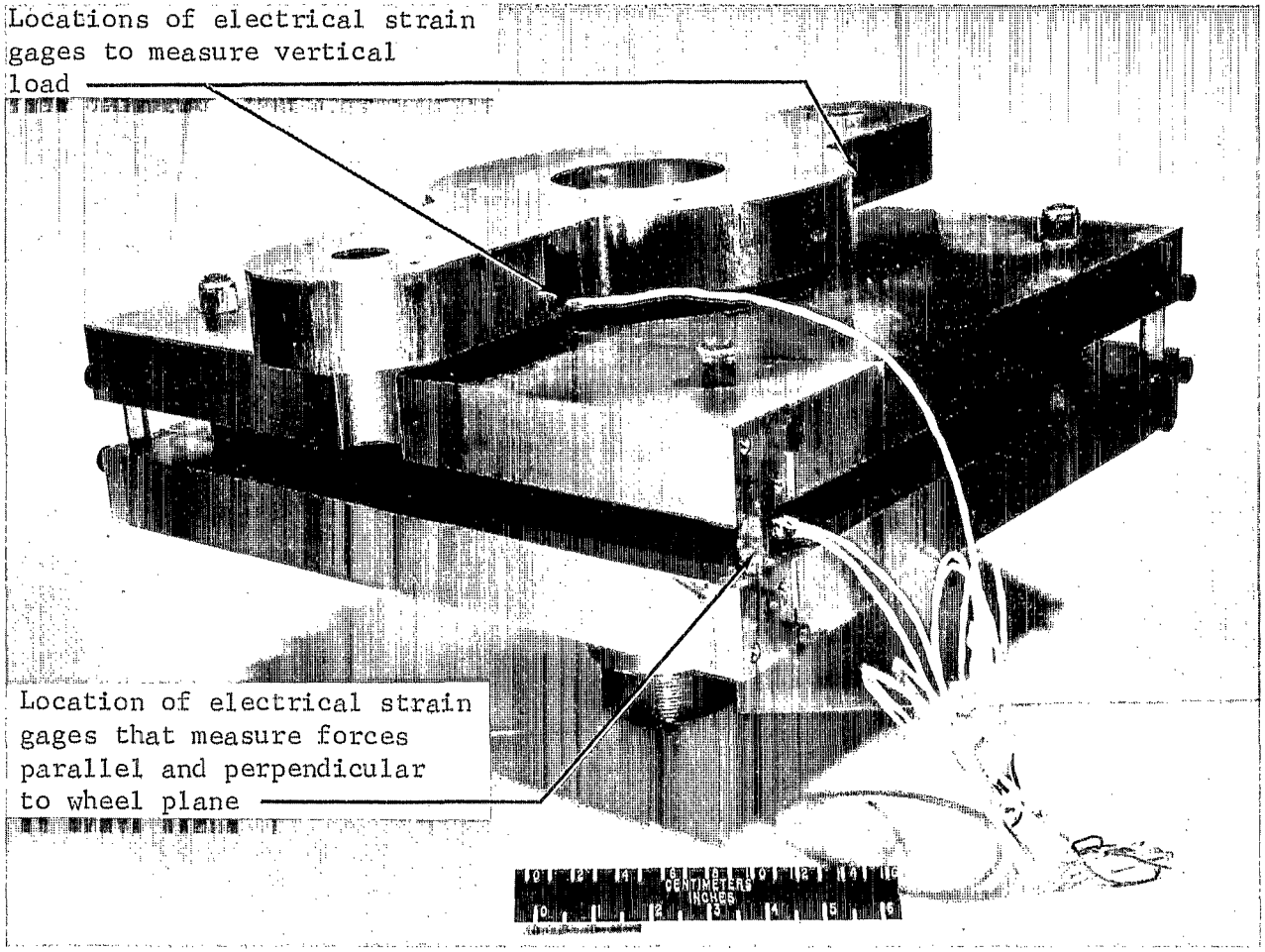

(e) Three-component force balance. L-68-846

Figure 1.- Concluded.

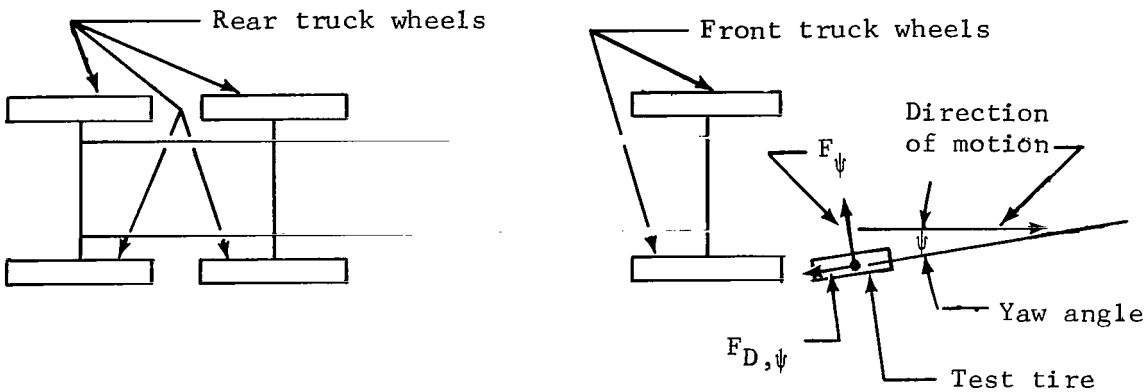

(a) Relative location of test and truck wheels.

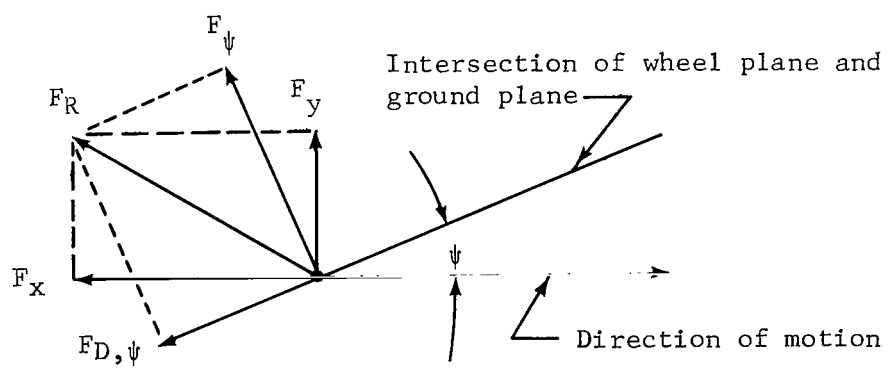

(b) Vector diagram of test-tire—ground contact forces.

Figure 2.- Schematic diagram of relative location of truck and test wheels and vector diagram of test-tire—ground contact forces.

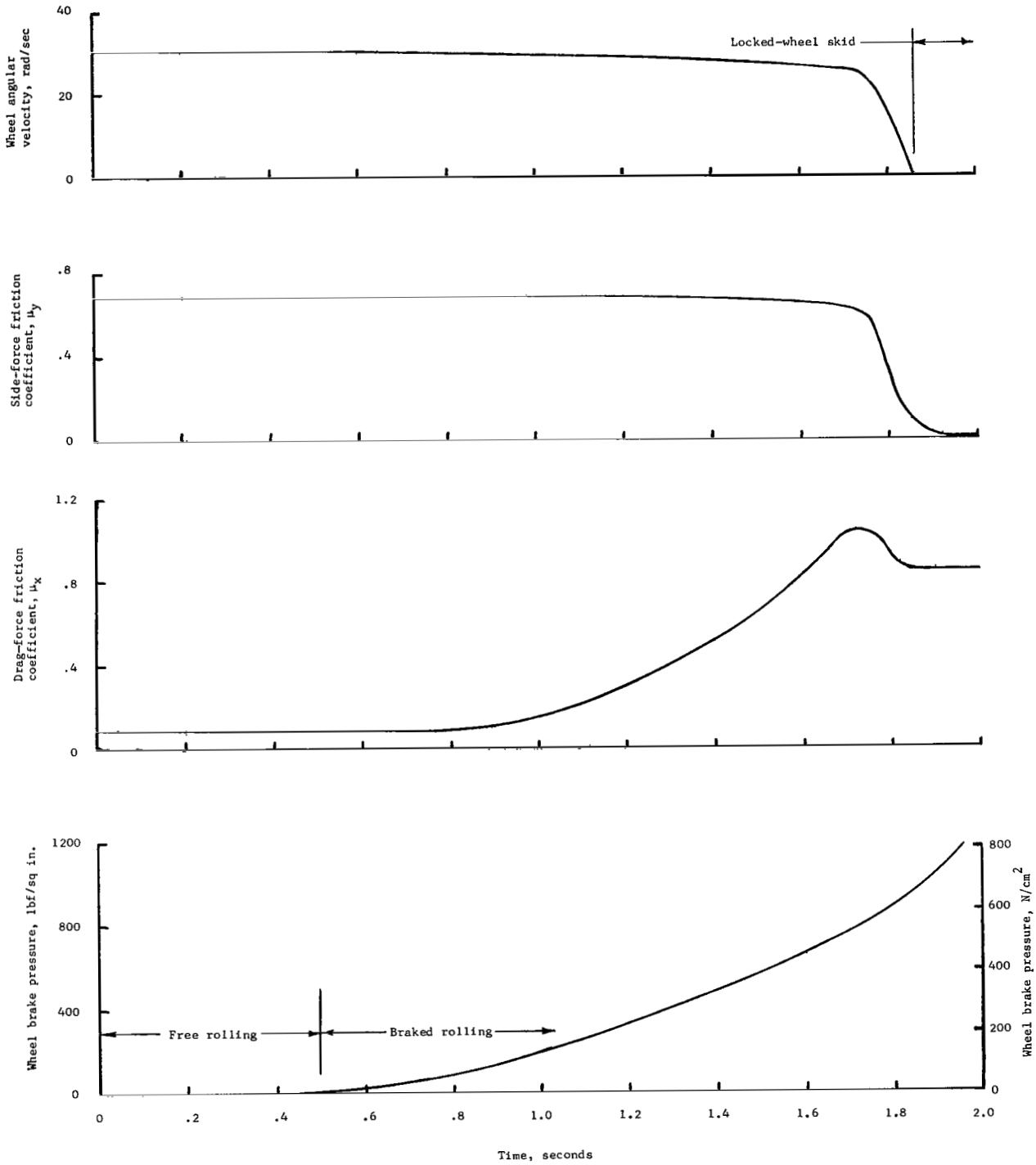

Figure 3.- Typical time histories of side- and drag-force friction coefficients, brake pressure, and wheel angular velocity obtained during wheel brake application on a dry concrete surface. Tire inflation pressure, 30 lbf/sq in. (20.7 N/cm^2); vertical load, 1000 lbf (4.45 kN); yaw angle, 4°; ground speed, 20 mph (17.4 knots).

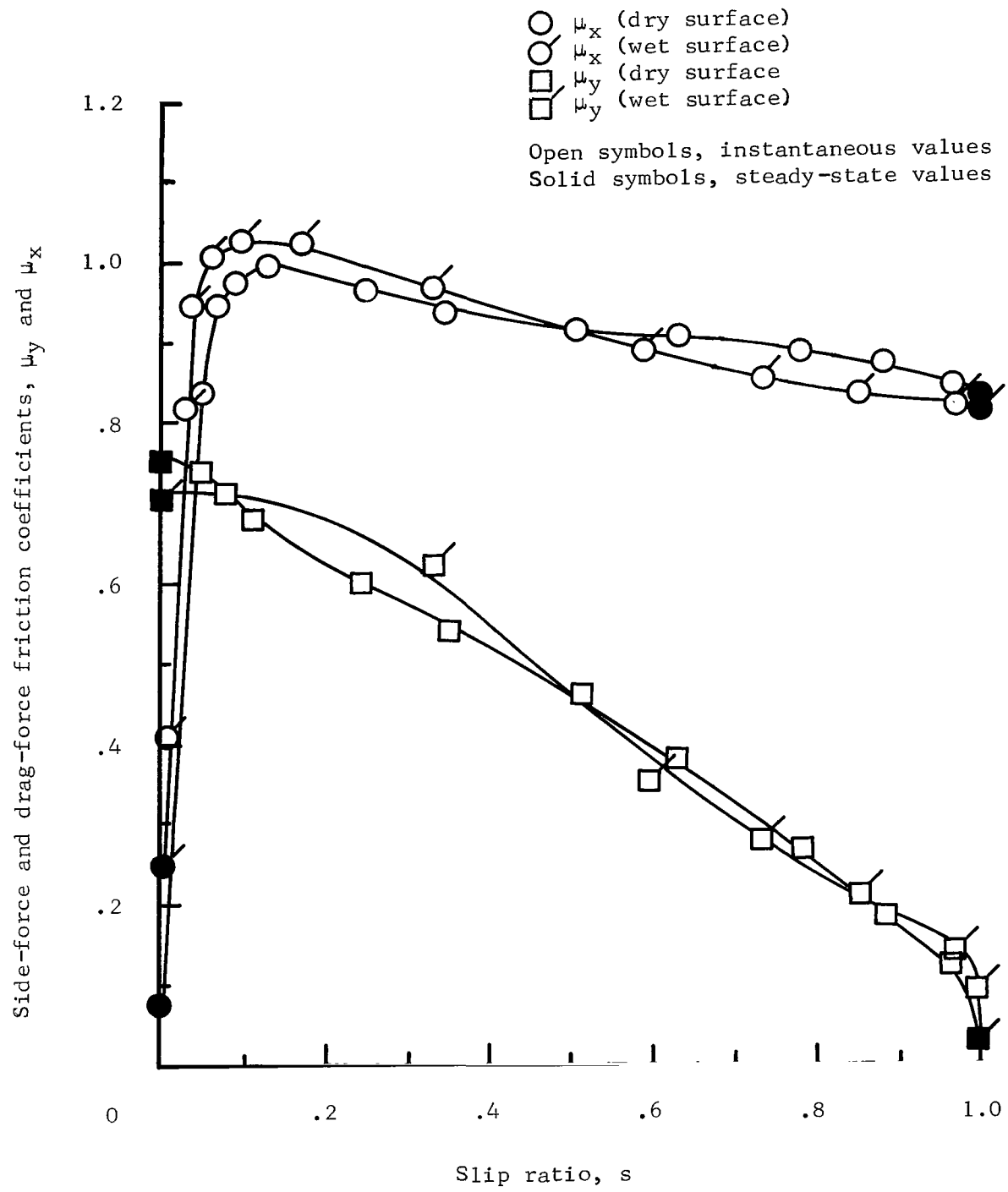

(a) V = 10 mph (8.7 knots).

Figure 4.- Variation of side- and drag-force friction coefficients obtained from yawed-rolling tests of a smooth-tread pneumatic tire undergoing brake application on wet and dry concrete pavements. Tire inflation pressure, 30 lbf/sq in. (20.7 N/cm^2); vertical load, 1000 lbf (4.45 kN); water depth, 0.5 in. (1.27 cm); yaw angle, 4°.

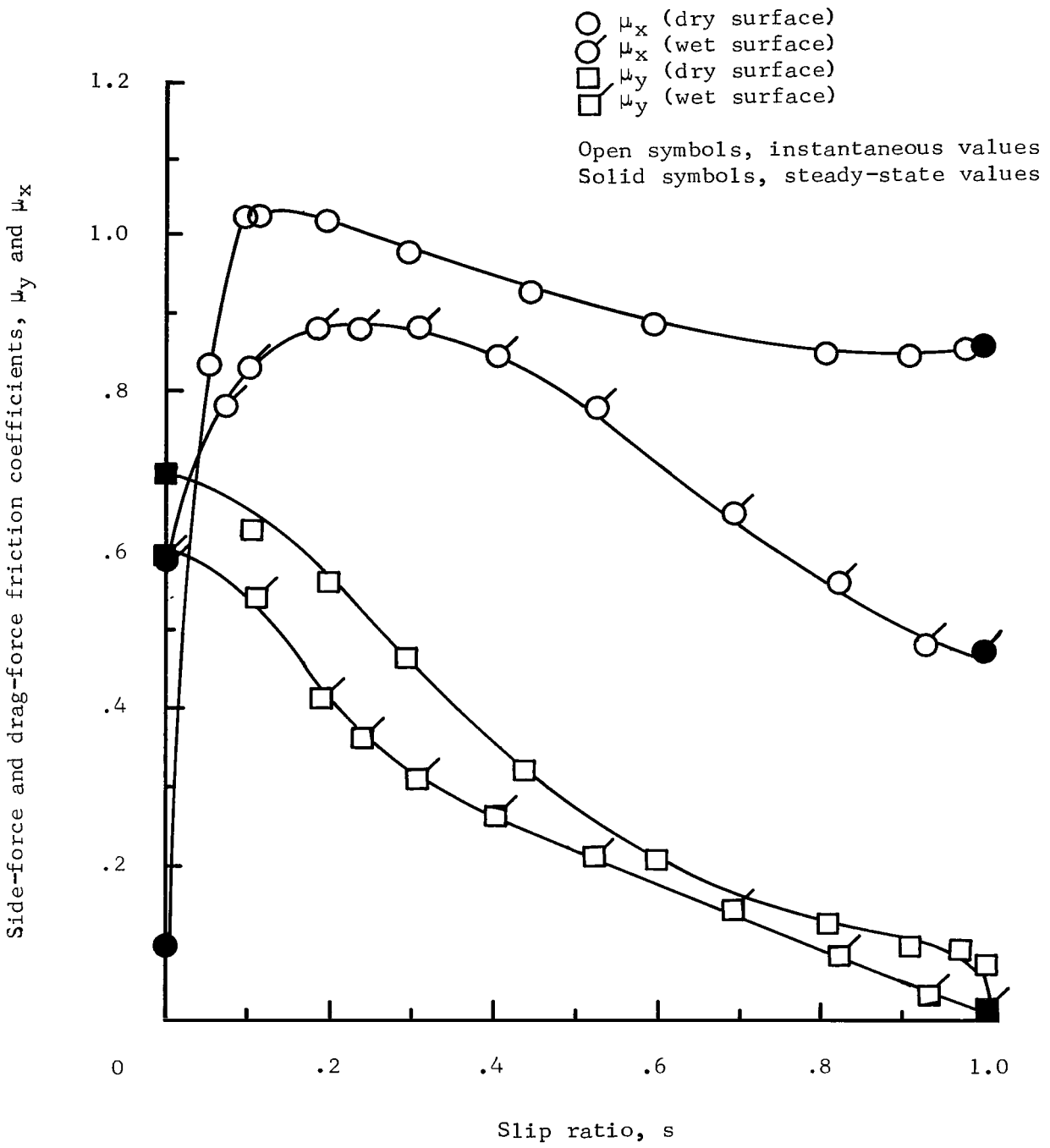

(b) V = 20 mph (17.4 knots).

Figure 4.- Continued.

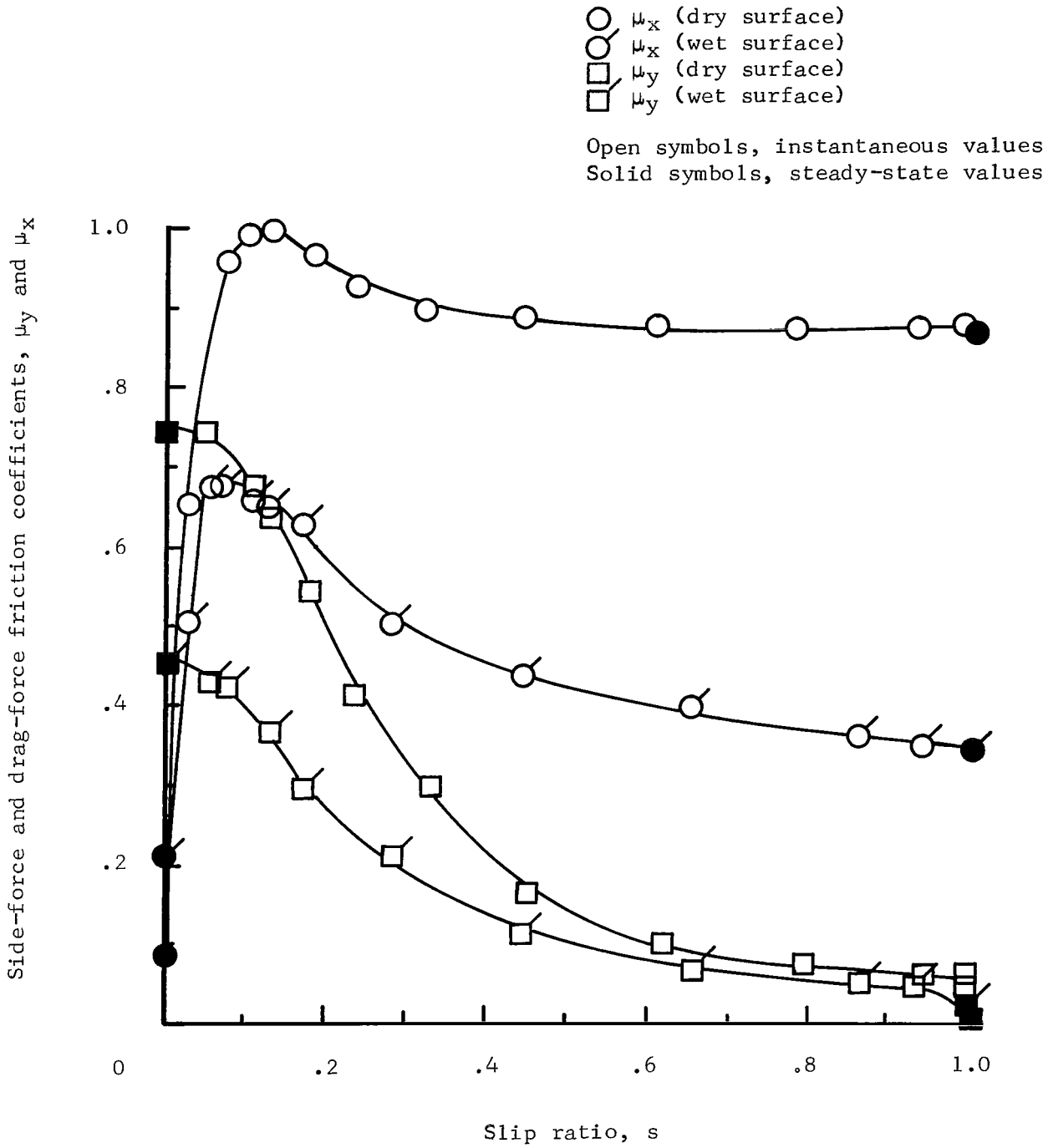

(c) V = 30 mph (26.1 knots).

Figure 4.- Concluded.

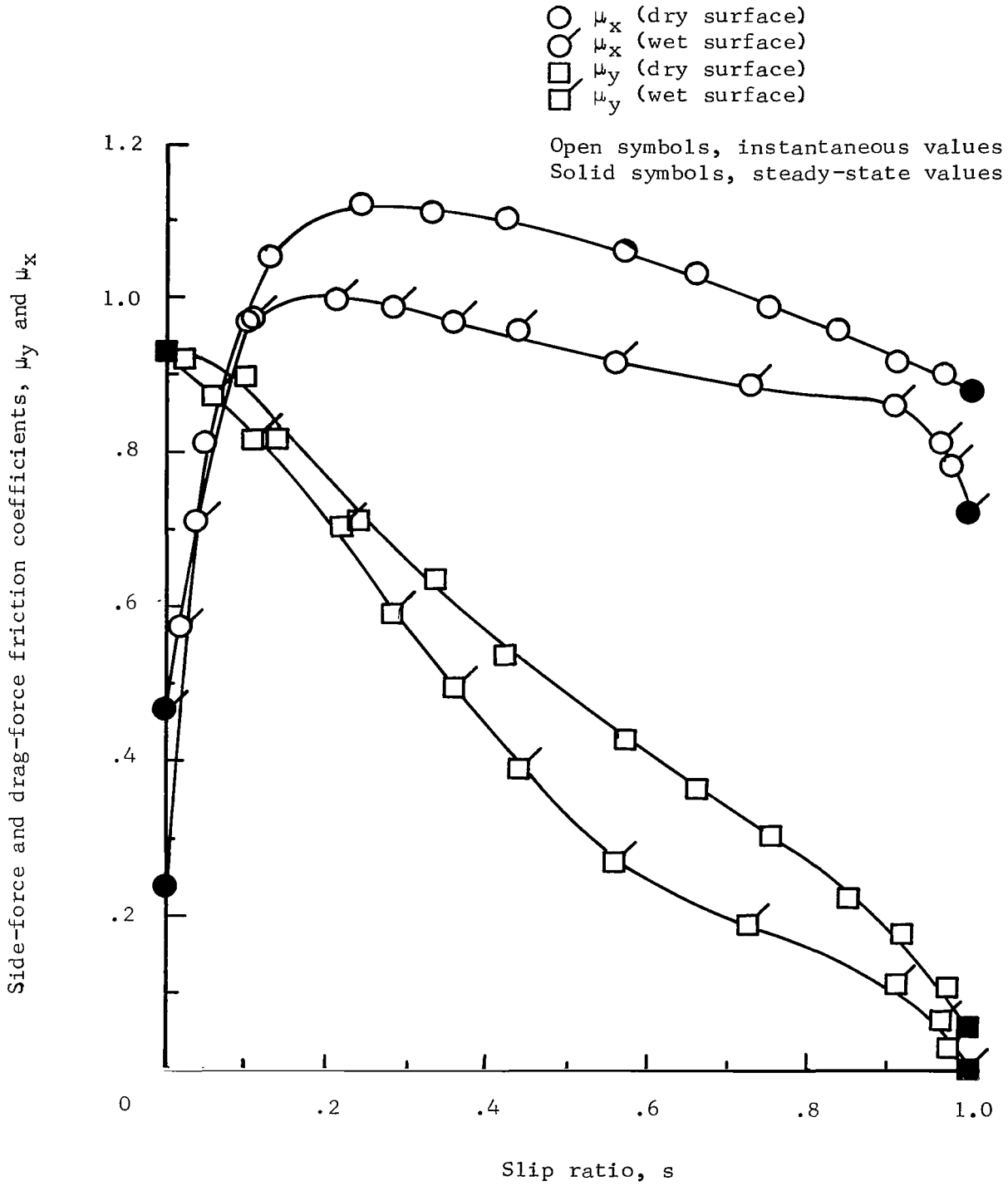

(a) V = 10 mph (8.7 knots).

Figure 5.- Variation of side- and drag-force friction coefficients obtained from yawed-rolling tests of a smooth-tread pneumatic tire undergoing brake application on wet and dry concrete pavements. Tire inflation pressure, 30 lbf/sq in. (20.7 N/cm^2); vertical load, 1000 lbf (4.45 kN); water depth, 0.5 in. (1.27 cm); yaw angle, 8^0.

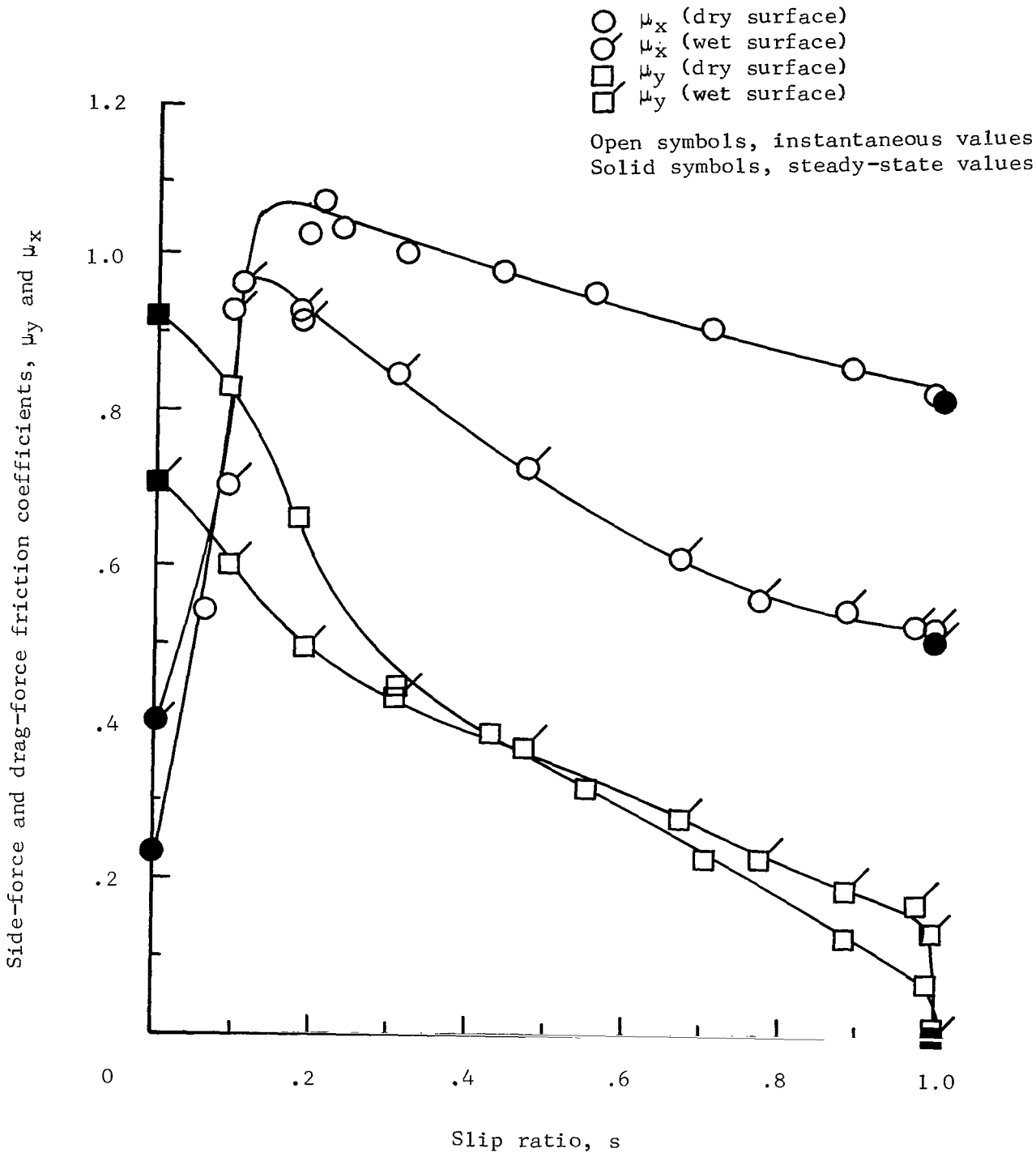

(b) V = 20 mph (17.4 knots).

Figure 5.- Continued.

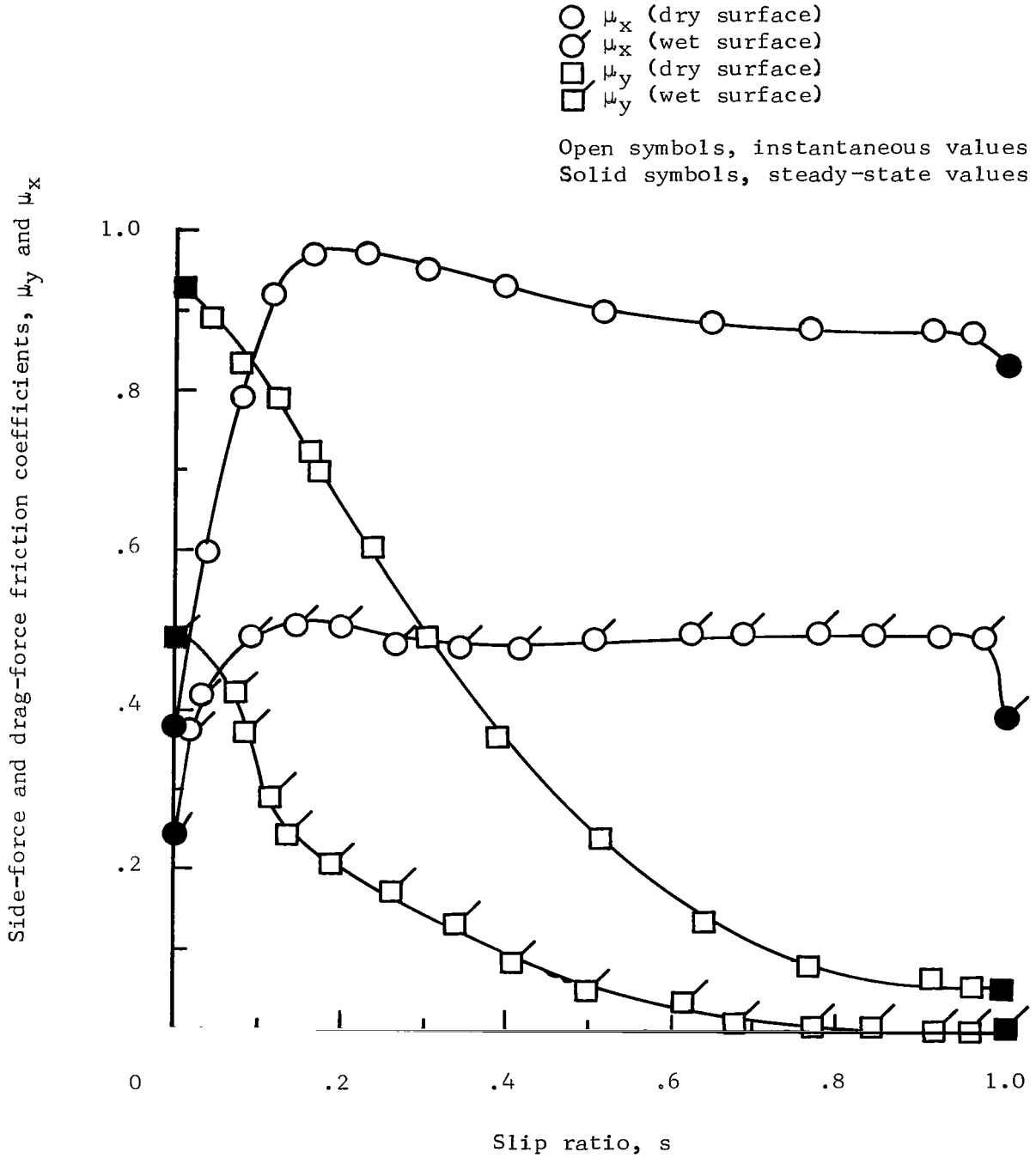

(c) V = 30 mph (26.1 knots).

Figure 5.- Concluded.

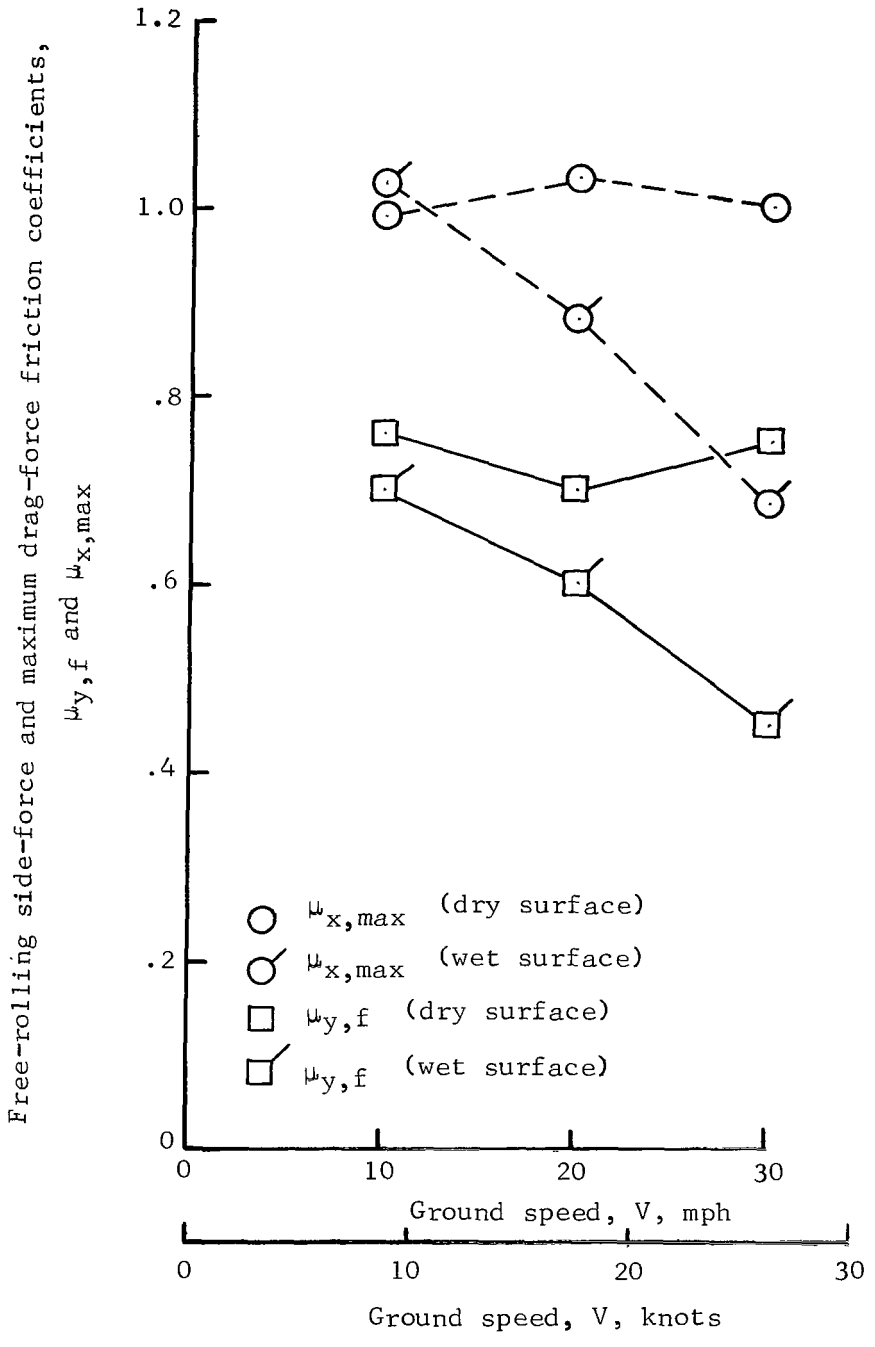

(a) $\psi = 4^0$.

Figure 6.- Variation of free-rolling side- and maximum drag-force coefficients with ground speed of a smooth-tread pneumatic tire on dry and wet concrete pavements. Tire inflation pressure, 30 lbf/sq in. (20.7 N/cm2); vertical load, 1000 lbf (4.45 kN); water depth, 0.5 in. (1.27 cm).

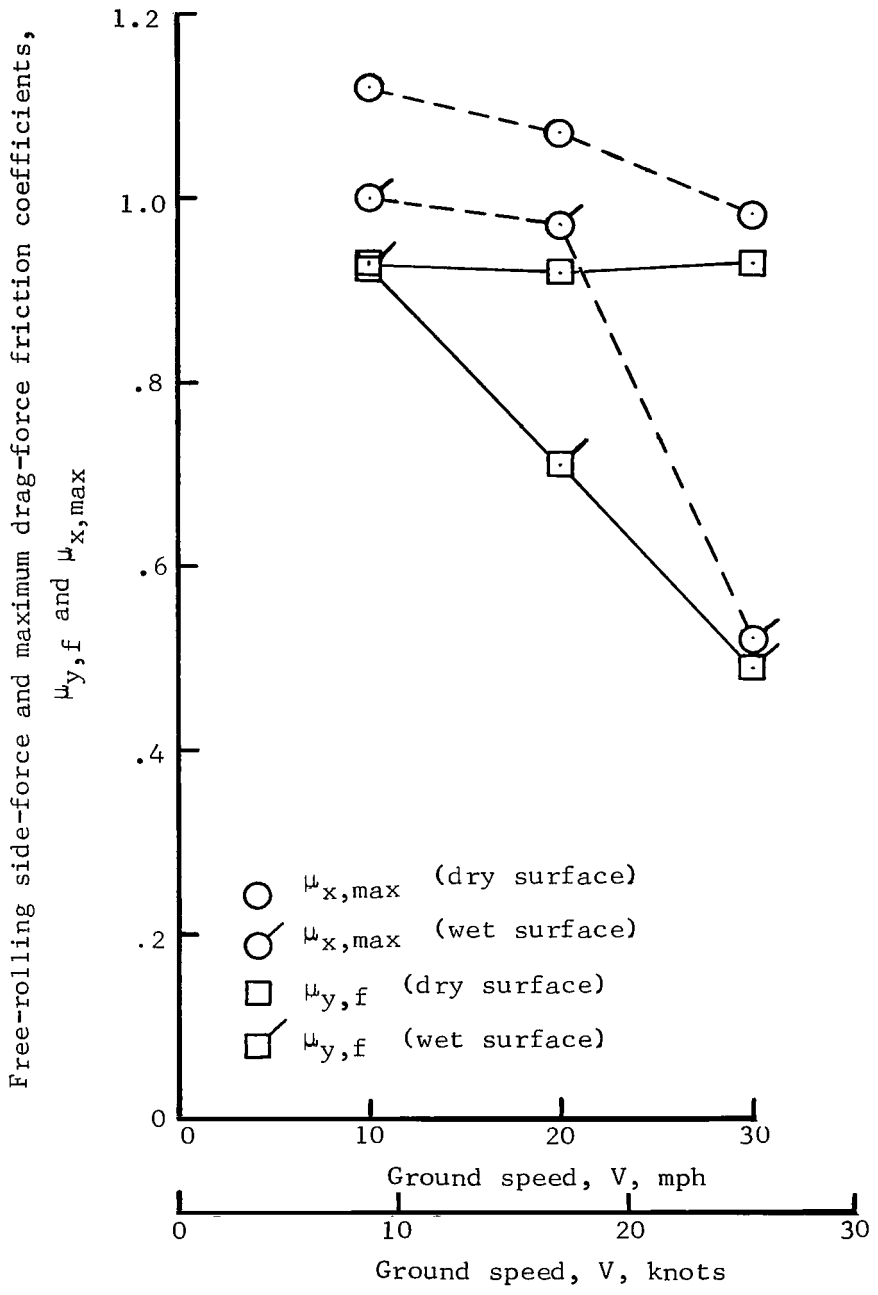

(b) $\psi = 8^0$.

Figure 6.- Concluded.

NATIONAL AERONAUTICS AND SPACE ADMINISTRATION
WASHINGTON, D. C. 20546

OFFICIAL BUSINESS

FIRST CLASS MAIL

POSTAGE AND FEES PAID
NATIONAL AERONAUTICS AND
SPACE ADMINISTRATION

POSTMASTER: If Undeliverable (Section 158 Postal Manual) Do Not Return

"The aeronautical and space activities of the United States shall be conducted so as to contribute . . . to the expansion of human knowledge of phenomena in the atmosphere and space. The Administration shall provide for the widest practicable and appropriate dissemination of information concerning its activities and the results thereof."

—NATIONAL AERONAUTICS AND SPACE ACT OF 1958

NASA SCIENTIFIC AND TECHNICAL PUBLICATIONS

TECHNICAL REPORTS: Scientific and technical information considered important, complete, and a lasting contribution to existing knowledge.

TECHNICAL NOTES: Information less broad in scope but nevertheless of importance as a contribution to existing knowledge.

TECHNICAL MEMORANDUMS: Information receiving limited distribution because of preliminary data, security classification, or other reasons.

CONTRACTOR REPORTS: Scientific and technical information generated under a NASA contract or grant and considered an important contribution to existing knowledge.

TECHNICAL TRANSLATIONS: Information published in a foreign language considered to merit NASA distribution in English.

SPECIAL PUBLICATIONS: Information derived from or of value to NASA activities. Publications include conference proceedings, monographs, data compilations, handbooks, sourcebooks, and special bibliographies.

TECHNOLOGY UTILIZATION PUBLICATIONS: Information on technology used by NASA that may be of particular interest in commercial and other non-aerospace applications. Publications include Tech Briefs, Technology Utilization Reports and Notes, and Technology Surveys.

Details on the availability of these publications may be obtained from:

SCIENTIFIC AND TECHNICAL INFORMATION DIVISION

NATIONAL AERONAUTICS AND SPACE ADMINISTRATION

Washington, D.C. 20546